AIP | Journal of Applied Physics

Forming delocalized intermediate states with realistic quantum dots

W. M. Reid, T. Driscoll, and M. F. Doty

Citation: J. Appl. Phys. **111**, 056102 (2012); doi: 10.1063/1.3691113
View online: http://dx.doi.org/10.1063/1.3691113
View Table of Contents: http://jap.aip.org/resource/1/JAPIAU/v111/i5
Published by the American Institute of Physics.

Forming delocalized intermediate states with realistic quantum dots

W. M. Reid,[1] T. Driscoll,[2] and M. F. Doty[1,a)]
[1]*Department of Materials Science and Engineering, University of Delaware, Newark, Delaware 19716, USA*
[2]*Department of Mathematical Sciences, University of Delaware, Newark, Delaware 19716, USA*

(Received 4 January 2012; accepted 23 January 2012; published online 8 March 2012)

Experiments and theoretical models suggest that the performance of intermediate band solar cells based on quantum dots (QDs) will be enhanced by the formation of delocalized intermediate bands. However, reasonable device performance has only been achieved when the QD separation is large and energy states are localized to individual QDs. In this paper we analyze the formation of delocalized bands in a realistic QD material that has inhomogeneously distributed energy levels. We calculate the QD uniformity or barrier thickness necessary to create delocalized states in realistic materials and propose a design to create delocalized states while including strain balancing layers. © *2012 American Institute of Physics*. [http://dx.doi.org/10.1063/1.3691113]

Intermediate band solar cells (IBSCs) incorporate a half-filled intermediate band (IB) located between the valence band (VB) and conduction band (CB) of a conventional single-junction solar cell.[1,2] Incorporation of the IB enables utilization of a wider portion of the solar spectrum; consequently, IBSCs are predicted to increase the theoretical maximum solar conversion efficiency under concentrated illumination from 40.7% to 63.2%.[3] A leading material system for fabricating IBSCs is densely packed vertically aligned arrays of self-assembled quantum dots (QDs), typically InAs, embedded in a III-V single-junction cell.[4,5] The arrays must contain approximately 50 periods of QDs to absorb enough photons, but growth of 50 closely spaced layers of QDs leads to accumulation of significant strain and the formation of lattice defects that degrade device performance.[6]

Theoretical models of IBSC devices assume that all QDs in the array have identical energy levels, enabling formation of fully delocalized energy bands by coherent tunneling between the QDs (see schematic in Fig. 1(a)).[6–10] There is both experimental and theoretical evidence to suggest that the formation of these delocalized bands will suppress phonon-mediated relaxation from the CB to the IB.[4,7,10,11] The existence of delocalized states is also a key element of existing theoretical approaches for calculating the optical transition dipoles and nonradiative relaxation rates between VB, IB, and CB levels.[10]

Although existing models assume identical QDs,[9,10] all known methods of QD growth yield an inhomogeneous distribution of QD energy levels. This distribution of energy levels can be seen clearly in the Gaussian distribution of QD photoluminescence (PL) energies.[6] Moreover, relatively thick barriers between QDs are needed to accommodate strain compensation layers[5,6] and suppress the thermal escape of electrons by phonon-assisted tunneling between QDs in a region with non-zero electric field, as depicted in Fig. 1(b).[12] As we now show, the inhomogeneously distributed QD energy levels of realistic materials prevent the formation of delocalized states when the QDs are separated by thick barriers. Our results quantify the improvements in QD uniformity and/or reductions in barrier thickness necessary to create spatially extended states. The results further reveal that identical QDs and delocalized states should not be assumed in realistic models of IBSC device photophysics.

We analyze the formation of delocalized states by solving the Schrödinger equation for arrays containing up to 50 QDs with varying inhomogeneous distributions of QD energy levels. We model the QD array in the growth direction as a one-dimensional superlattice and capture the fluctuations in energy levels by varying the depth of the potential well for each QD. The Schrödinger equation for our system is

$$-\frac{\hbar^2}{2m^*}\frac{d^2\Psi(x)}{dx^2}+V(x)\Psi(x)=\varepsilon\Psi(x), \tag{1}$$

where $\Psi(x)$ is the wave function, $\hbar$ is Planck's constant, and m^* is the electron effective mass (0.067 in GaAs, 0.022 in InAs). The potential energy profile $V(x)$ includes the GaAs barrier height (0.85 eV), barrier width, and the width of the QD potential (6.5 nm). The depth of each QD potential well is randomly selected from a Gaussian distribution centered on 0 with a specified standard deviation, σ. This replicates the consequences of random alloying and size variation in each QD and results in a distribution of energy levels among the QDs. Existing growth protocols result in a distribution of energy levels of approximately 0.0565 eV, which we label σ_0.[6] The array of QDs is placed between thick GaAs barriers, simulating the conditions of prototype devices.

We numerically solve the Schrödinger equation using Chebyshev spectral collocation methods implemented by the Chebfun Matlab package.[13,14] We calculate all wavefunctions ($\Psi(x)$) composed of QD ground states by finding the n solutions of lowest energy in an array of n QDs. We then calculate the probability amplitude ($\Psi^2(x)$) for each wavefunction. Figure 2(a) shows the potential profile and calculated probability amplitude for three QDs located in the middle of an array containing 30 identical QDs separated by 3 nm GaAs barriers. Because the QDs are identical ($\sigma=0$), the

a)Electronic mail: doty@udel.edu.

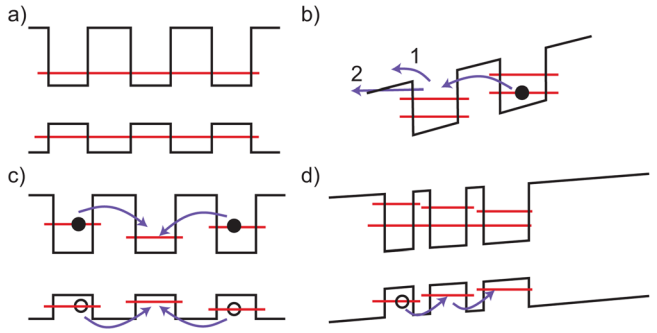

FIG. 1. (Color online) (a) Schematic of delocalized bands formed in identical QDs. (b) Escape of electrons from QDs in an applied field via thermal (1) or tunneling (2) processes. (c) Thermal relaxation processes in arrays of closely spaced realistic QDs. (d) Delocalization over a few QDs can be achieved in a cluster of closely spaced QDs.

wavefunctions have a maximum probability amplitude that is constant over all QDs, equivalent to the minibands of a finite superlattice. In Fig. 2(b), the QD potentials are randomly distributed with width σ_0. As a result of the inhomogeneous distribution of energy levels, coherent tunneling is suppressed and the wavefunctions are localized in individual QDs. In Fig. 2(c) we plot the periodic potential and probability amplitudes for QDs separated by 10 nm barriers, representative of the barrier thickness required to accommodate strain-balancing layers. Because the coherent tunneling falls off exponentially with the thickness of the barrier, the wavefunctions are localized to individual QDs, despite the fact that the width of the QD potential distribution used in the

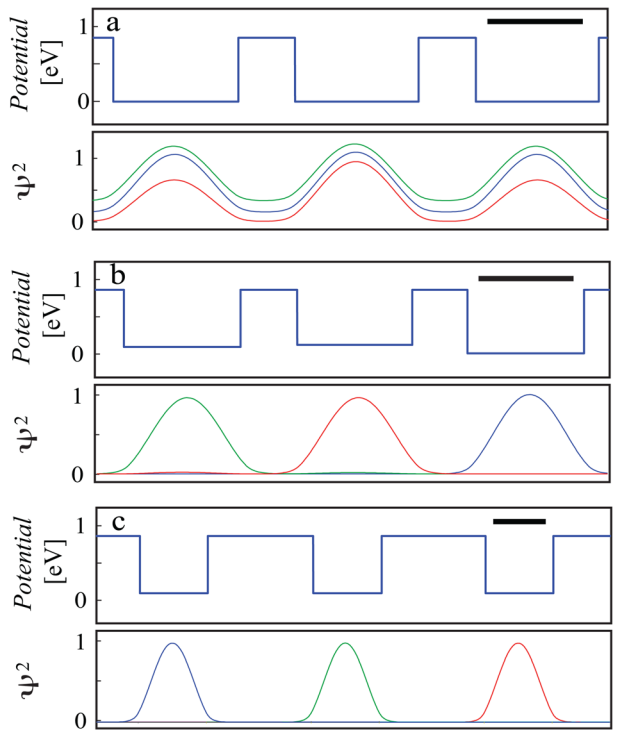

FIG. 2. (Color online) (a) Delocalized wavefunctions in identical QDs separated by 3 nm GaAs barriers. The top two curves are offset for clarity. The thick black line in all panels is 5 nm long. (b) Localized wavefunctions in nonidentical QDs separated by 3 nm barriers with $\sigma = \sigma_0$. (c) Localized wavefunctions in nonidentical QDs separated by 10 nm barriers with $\sigma = \sigma_0/10^3$.

calculation of Fig. 2(c) is $\sigma_0/10^3$, three orders of magnitude narrower than the distribution presently achievable.[6,15]

The calculations presented in Fig. 2 demonstrate that arrays of realistic QDs separated by barriers as small as 3 nm must be viewed as a series of localized states. The existence of localized states must induce deviations from the rates of optical excitation and nonradiative relaxation predicted for delocalized bands.[10] The localized states also create pathways for phonon-assisted tunneling that funnel multiple carriers to a single QD (Fig. 1(c)), increasing the probability of Auger thermal relaxation.[16]

We assess the uniformity of QD energy levels necessary to achieve delocalized bands by calculating the average spatial extent of wavefunctions (the average localization length, ξ) as a function of σ. To determine ξ, we first determine the QD on which each wavefunction is centered (i.e., the location of the maximum of each Ψ^2). We then calculate the number of QDs that contain a wavefunction amplitude (Ψ^2) at least 10% of the maximum amplitude. We assess the importance of this 10% cut-off amplitude by repeating all calculations using a 1% cut-off amplitude. We independently calculate ξ for all n ground-state wavefunctions in a single realization of the random potential profile of n QDs. We then repeat this process for 5 separate realizations of the random QD potential. The average and standard deviation of ξ is calculated using all the wavefunctions in all random realizations that have the same σ and QD separation.

In Fig. 3(a), we plot ξ versus σ for QDs separated by 10 nm and 3 nm barriers using both a 10% (open symbols) and 1% (closed symbol) cut-off amplitude. ξ is presented in units of the number of QDs over which the wavefunction is extended. When QDs are separated by 10 nm barriers (diamonds), we find that delocalized states are not formed until σ drops below $\sigma_0/10^4$. Wavefunctions delocalized over nearly 50 QDs do not occur until energy distributions approach $\sigma_0/10^5$. When the barrier thickness is reduced to 3 nm (circles), the increased tunneling strength due to the thinner barriers allows the formation of wavefunctions delocalized over several QDs when $\sigma = \sigma_0/10$. Achieving a wavefunction that is delocalized over nearly 50 QDs requires $\sigma = \sigma_0/10^2$. We find that considering a 1% cut-off fraction (closed symbols) relaxes the σ required to form delocalized states by a factor of about 2 for both the 3 and 10 nm case. Consequently, we conclude that the exact value of the cut-off amplitude does not impact our overall result: when QDs are separated by barriers of 3 nm or more, the formation of wavefunctions delocalized over nearly 50 QDs requires a distribution of QD energy levels at least two orders of magnitude narrower than produced by current growth methods.

Although there are techniques for narrowing the QD energy level distribution, including annealing and growing on pre-patterned substrates, improving uniformity by 2 to 5 orders of magnitude is an extraordinary and likely insurmountable challenge because the self-assembly of InAs QDs involves diffusion, which is inherently random. We therefore analyze the separation of QDs necessary to create delocalized states with realistic distributions of QD energy levels (σ_0). In Fig. 3(b) we plot the average localization length (ξ) as a function of barrier thickness. The results reveal that

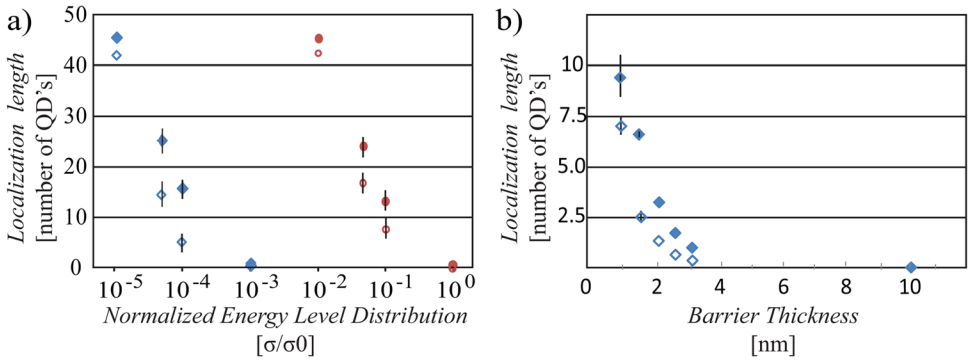

FIG. 3. (Color online) (a) Localization length plotted as a function of σ for 50 QDs separated by 3 nm barriers (circles) and 10 nm barriers (diamonds). The spatial extent is calculated using both a 10% (open) and 1% (solid) cut-off for the probability amplitude. (b) Localization length plotted as a function of barrier thickness for presently achievable values of the QD homogeneity (σ_0).

electron wavefunctions delocalized over at least 5 QDs can be achieved when the QDs are separated by barriers of 1.5 nm or less.

Present models of IBSC devices suggest that fully delocalized IB states are ideal, but there are no experimental measurements of the relationship between nonradiative relaxation rates and the spatial extent of wavefunctions in InGaAs QDs. It is possible that delocalization over just a few QDs is sufficient to reduce nonradiative recombination to a level acceptable for device performance. A possible architecture that creates states delocalized over several QDs while preserving the possibility of including strain-compensation layers is depicted in Fig. 1(d). This design is based on clusters of QDs rather than a symmetric array. The QDs within each cluster are separated by very thin barriers, enabling the formation of spatially extended states.[17] Although there will be significant strain accumulation within the cluster, the clusters can be separated by thick barrier regions that include strain compensation layers and prevent the net accumulation of strain.

Although the electron levels of QDs within such a cluster will form spatially extended states, the hole levels will remain localized due to the higher hole effective mass. To reduce the probability of Auger relaxation processes associated with holes,[16] the height of the QDs can be controlled using cap and flush methods.[15] As depicted in Fig. 1(d), placing a cluster of QDs with increasing height into a gently increasing potential can be used to tune the electron levels into resonance while detuning the hole energy levels.[15] The holes consequently relax to the lowest energy VB state in the right QD, while the electrons remain in delocalized states. The intentional use of nonidentical QDs provides a deterministic method for controlling the spatial extent of the electron wavefunctions, the spatial overlap of electrons and holes, and the thermal escape of carriers.

Our computational results reveal that fully delocalized bands in arrays of self-assembled QDs cannot be achieved without improbable advances in growth uniformity. It is feasible, however, to create spatially extended states in small clusters of QDs separated by very thin barriers. The QD cluster approach provides a great deal of flexibility in designing QD arrays with tailored wavefunctions, optical properties, and thermal relaxation properties. The design of an optimal QD cluster architecture, however, requires both experimental and theoretical studies of the relationship between spatially extended states and electron and hole recombination and relaxation processes.

[1]A. Luque and A. Marti, Adv. Mater. **22**, 160 (2010).
[2]N. Lopez, L. Reichertz, K. Yu, K. Campman, and W. Walukiewicz, Phys. Rev. Lett. **106**, 028701 (2011).
[3]A. Luque and A. Mart, Phys. Rev. Lett. **78**, 5014 (1997).
[4]A. Luque, P. G. Linares, E. Antolin, E. Canovas, C. D. Farmer, C. R. Stanley, and A. Marti, Appl. Phys. Lett. **96**, 3 (2010).
[5]C. Bailey, D. Forbes, R. Raffaelle, and S. Hubbard, Appl. Phys. Lett. **98**, 163105 (2011).
[6]V. Popescu, G. Bester, M. C. Hanna, A. G. Norman, and A. Zunger, Phys. Rev. B **78**, 205321 (2008).
[7]A. Luque, A. Marti, E. Antolin, and C. Tablero, Physica B **382**, 320 (2006).
[8]S. Tomic, T. S. Jones, and N. M. Harrison, Appl. Phys. Lett. **93**, 263105 (2008).
[9]C. G. Bailey, S. M. Hubbard, D. V. Forbes, R. Aguinaldo, C. D. Cress, S. J. Polly, and R. P. Raffaelle, paper presented at the *2009 34th IEEE Photovoltaic Specialists Conference (PVSC)*, Philadelphia, PA, 7–12 June 2009.
[10]S. Tomic, Phys. Rev. B **82**, 195321 (2010).
[11]E. Antolin, A. Marti, J. Olea, D. Pastor, G. Gonzalez-Diaz, I. Martil, and A. Luque, Appl. Phys. Lett. **94**, 3 (2009).
[12]E. Antolin, A. Marti, P. G. Linares, I. Ramiro, E. Hernańdez, C. D. Farmer, C. R. Stanley, and A. Luque, paper presented at the *2010 35th IEEE Photovoltaic Specialists Conference (PVSC)*, Honolulu, HI, 20–25 June 2010.
[13]T. Driscoll, F. Bornemann, and L. Trefethen, BIT Numer. Math. **48**, 701 (2008).
[14]A. Birkisson and T. Driscoll, "Automatic Fréchet differentiation for the numerical solution of boundary-value problems," ACM Trans. Math. Softw. (submitted).
[15]A. S. Bracker, M. Scheibner, M. F. Doty, E. A. Stinaff, I. V. Ponomarev, J. C. Kim, L. J. Whitman, T. L. Reinecke, and D. Gammon, Appl. Phys. Lett. **89**, 233110 (2006).
[16]S. Tomic, A. Mart, E. Antoln, and A. Luque, Appl. Phys. Lett. **99**, 053504 (2011).
[17]Y. Nakata, Y. Sugiyama, T. Futatsugi, and N. Yokoyama, J. Cryst. Growth **175**, 713 (1997).